



Injection of Vessel-Derived Stem Cells Prevents Dilated Cardiomyopathy and Promotes Angiogenesis and Endogenous Cardiac Stem Cell Proliferation in *mdx/utrn*^{-/-} but Not Aged *mdx* Mouse Models for Duchenne Muscular Dystrophy

JU LAN CHUN,^a ROBERT O'BRIEN,^b MIN HO SONG,^a BLAKE F. WONDASCH,^c SUZANNE E. BERRY^{c,d,e}

Key Words. Cellular therapy • Muscular dystrophy • Angiogenesis • Cardiac • Cellular proliferation • Neural stem cell • Cell transplantation

^aDepartment of Animal Sciences, ^bDepartment of Veterinary Clinical Medicine, ^cDepartment of Comparative Biosciences, ^dInstitute for Genomic Biology, and ^eNeuroscience Program, University of Illinois, Urbana, Illinois, USA

Correspondence: Suzanne E. Berry, Ph.D., Department of Comparative Biosciences, 3812 VMBSB, 2001 South Lincoln Avenue, University of Illinois at Urbana-Champaign, Urbana, Illinois 61802, USA. Telephone: 217-333-4246; Fax: 217-244-1652; E-Mail: berryse@illinois.edu

Received August 30, 2012; accepted for publication October 29, 2012; first published online in *SCTM EXPRESS* December 27, 2012.

©AlphaMed Press
1066-5099/2012/\$20.00/0

<http://dx.doi.org/10.5966/sctm.2012-0107>

ABSTRACT

Duchenne muscular dystrophy (DMD) is the most common form of muscular dystrophy. DMD patients lack dystrophin protein and develop skeletal muscle pathology and dilated cardiomyopathy (DCM). Approximately 20% succumb to cardiac involvement. We hypothesized that mesoangioblast stem cells (aorta-derived mesoangioblasts [ADMs]) would restore dystrophin and alleviate or prevent DCM in animal models of DMD. ADMs can be induced to express cardiac markers, including Nkx2.5, cardiac tropomyosin, cardiac troponin I, and α -actinin, and adopt cardiomyocyte morphology. Transplantation of ADMs into the heart of *mdx/utrn*^{-/-} mice prior to development of DCM prevented onset of cardiomyopathy, as measured by echocardiography, and resulted in significantly higher CD31 expression, consistent with new vessel formation. Dystrophin-positive cardiomyocytes and increased proliferation of endogenous Nestin⁺ cardiac stem cells were detected in ADM-injected heart. Nestin⁺ striated cells were also detected in four of five *mdx/utrn*^{-/-} hearts injected with ADMs. In contrast, when ADMs were injected into the heart of aged *mdx* mice with advanced fibrosis, no functional improvement was detected by echocardiography. Instead, ADMs exacerbated some features of DCM. No dystrophin protein, increase in CD31 expression, or increase in Nestin⁺ cell proliferation was detected following ADM injection in aged *mdx* heart. Dystrophin was observed following transplantation of ADMs into the hearts of young *mdx* mice, however, suggesting that pathology in aged *mdx* heart may alter the fate of donor stem cells. In summary, ADMs delay or prevent development of DCM in dystrophin-deficient heart, but timing of stem cell transplantation may be critical for achieving benefit with cell therapy in DMD cardiac muscle. *STEM CELLS TRANSLATIONAL MEDICINE* 2013;2:000–000

INTRODUCTION

Duchenne muscular dystrophy (DMD) is an X-linked fatal muscle wasting disease affecting approximately 1 in every 3,500 boys born [1]; it results from mutations in the dystrophin gene. Patients exhibit severe, progressive pathology in skeletal muscle, as well as dilated cardiomyopathy (DCM). The incidence of DMD patients developing cardiomyopathy has increased. Medical advances in the past decade, including positive pressure ventilation and surgery for spinal fusion, have significantly extended the life span of patients, and as a result, nearly all DMD patients now develop DCM [2–7].

Currently, angiotensin-converting enzyme (ACE) inhibitors, beta blockers, and steroids have been beneficial for treating the symptoms of dystrophin-deficient cardiomyopathy in DMD patients. ACE inhibitors alone delayed loss of car-

diac function [8], normalized systolic dysfunction [9], and extended life [10]. Treatment with the beta blockers improved heart function and decreased tachycardia [11], and combined treatment with both ACE inhibitors and beta blockers increased heart function [12–15], reduced ventricular dilation [14, 15], and improved survival when given prior to an observed decrease in heart function [16]. Steroid treatment has also been effective, resulting in fewer patients with a decline in heart function [17–20] and decreased incidence of dilated cardiomyopathy [21]. ACE inhibitors, beta blockers, and steroids are therefore currently the standard of care for cardiomyopathy in DMD.

Another promising method of treatment is the use of membrane sealant to stabilize cardiomyocyte cell membranes in the absence of dystrophin. This has been shown to protect the heart

of DMD animal models from dobutamine-induced stress [22] and isoproterenol-induced cardiomyopathy [2] and to prevent left ventricular remodeling and reduce fibrosis in a canine model of Duchenne muscular dystrophy [23].

Although the aforementioned treatments have benefit in the heart and may delay cardiomyopathy, they do not address the underlying absence of dystrophin or loss of cardiomyocytes. Restoration of dystrophin protein and/or replacement of lost or damaged cardiomyocytes are necessary to prevent or reverse ventricular remodeling and pathology in dystrophin-deficient heart. A combination of the previous strategies, in addition to gene or cell therapy, may therefore offer the best potential outcome for DMD patients, as well as for patients with Becker muscular dystrophy, who have partially functional dystrophin protein, and patients with X-linked cardiomyopathy, who have lost dystrophin expression only in cardiac muscle [24–27].

Multiple approaches have been investigated to restore dystrophin in the heart of animal models for DMD. Viral delivery of a mini-dystrophin gene by recombinant adeno-associated virus (rAAV) restored dystrophin in mouse models of DMD [28, 29], improving heart function and protecting the heart during a dobutamine stress test [28]. However, the microdystrophin gene tested cannot fully compensate for dystrophin protein function in cardiac muscle [30, 31], and some viral vectors invoke an immune response in canine and human muscle [32–35]. Exon skipping is an alternative approach to restoring a functional dystrophin protein and has resulted in functional benefit in vivo [36], but would be useful only for patients with specific types of dystrophin mutations.

Cell therapy with transplantation of exogenous stem cells is another mechanism for restoring dystrophin and brings the added benefit of generation of new muscle cells to replace lost or damaged endogenous cells. We and others have shown that stem cells with a functional copy of the dystrophin gene can restore dystrophin expression to skeletal muscle of dystrophin-deficient mice [37] and dogs [38]. Only two studies have been conducted to determine whether stem cells will replace damaged cardiomyocytes or provide functional benefit in dystrophin-deficient cardiac muscle. Koh et al. [39] injected fetal cardiomyocytes into the heart of *mdx* mice and dystrophic dogs, which restored dystrophin in the heart and formed gap junctions for electrical coupling with host myocardium. However, the use of fetal human stem cells is controversial, and these cells would likely be difficult to obtain for use in the clinic. In another study, Payne et al. [40] have injected skeletal muscle-derived stem cells (MDSCs) into the heart of the *mdx* mouse model for DMD. MDSCs expressed dystrophin, but many remained committed to a skeletal muscle phenotype after transplantation, indicating that additional studies need to be conducted to find an alternative source of stem cells for therapy in dystrophin-deficient heart.

In the current study, we have injected aorta-derived mesoangioblasts (ADMs) with a functional copy of the dystrophin gene into the wall of the heart of murine models for DMD and determined whether they restored dystrophin expression and prevented or alleviated cardiomyopathy. Dystrophin-deficient *mdx* mice develop pathology in the heart and ventricular dilation between 12 and 21 months of age [41–43], and because of the near-normal life expectancy of the strain, long-term studies are possible. However, given the extended time necessary for development of cardiac pathology [42, 43], the broad range of time

when cardiomyopathy may develop [42, 43], and variation in the severity of cardiac pathology among mice in the *mdx* strain [41], we have also used *mdx/utrn*^{-/-} mice for our study. *mdx/utrn*^{-/-} mice are deficient in both dystrophin and utrophin, a homolog of dystrophin that functionally compensates for dystrophin in mice [44], and have severe, progressive skeletal muscle pathology and damaged, necrotic cardiomyocytes [45]. We recently reported that *mdx/utrn*^{-/-} mice develop DCM similar to DMD patients by 15 weeks of age [46]. Although *mdx/utrn*^{-/-} mice have a shortened life span, the consistent development and rapid onset of cardiomyopathy make them an ideal model for short-term preclinical studies using our stem cells. ADMs are myogenic in vitro and in vivo and have been used to restore dystrophin up to 50% of wild-type levels in the skeletal muscle of the *mdx/utrn*^{-/-} mouse, resulting in an approximately 50-fold decrease in damaged muscle fibers following transplantation [37]. We now report that ADMs can also be induced to express cardiac markers in vitro, delay onset of DCM, and promote unexpected changes in the heart that may contribute to functional benefit.

MATERIALS AND METHODS

Cell Culture

Clonally derived populations of ADMs were used for the study. ADMs were isolated from C57Bl/10 mice as previously described from explant cultures and characterized for their ability to differentiate into smooth and skeletal muscle cells in vitro and in vivo [37], and the marker profile of the cells has previously been reported (CD34⁺, Sca1⁺, CD90.1⁺, CD31⁻, CD45⁻, CD13⁻, CD146⁻) [47]. ADMs were cultured in Iscove's Dulbecco modified Eagle's minimal essential medium (DMEM) containing 20% fetal bovine serum (FBS), 0.1 U/ml penicillin, 0.1 μg/ml streptomycin, 2.0 mM L-glutamine, 0.1 mM nonessential amino acids, minimal essential medium vitamin solution from Gibco (Carlsbad, CA, <http://www.invitrogen.com>), and 20 ng/ml purified leukemia inhibitory factor (LIF) (Chemicon, Temecula, CA, <http://www.chemicon.com>), hereafter referred to as proliferation medium. The cells were expanded on 0.1% gelatin-coated plates and maintained in a humidified incubator at 37°C in 5% CO₂. Rat primary cardiomyocytes from neonate rat heart (ventricle) (catalog no. R6200; ScienCell Research Laboratories, San Diego, CA, <http://www.sciencellonline.com>) were cultured in DMEM containing 5% FBS and maintained at 37°C in 5% CO₂.

In Vitro Cardiomyocyte Differentiation

ADMs and rat primary cardiomyocytes (RCs) were seeded on glass coverslips coated with 0.1% gelatin in proliferation medium (ADMs) or DMEM containing 5% FBS (RCs, company recommendation). After cells attached, differentiation medium was added to ADMs, whereas rat cardiomyocytes were maintained in DMEM with 5% FBS. Differentiation medium included (a) DMEM containing 2% horse serum, (b) DMEM supplemented with 5% FBS and Cardiomyocyte Growth Supplement (100×) (ScienCell Research Laboratories, catalog no. 6252), and (c) DMEM supplemented with 10 μl/ml NDiff Neuro-2 Supplement (200×) (catalog no. SCM012; Chemicon) and 20 μl/ml B27 serum-free supplement (50×) (catalog no. 17504-044; Gibco). Cells were maintained in these conditions for 14 days, with medium

changes every other day. Images were also acquired every other day.

Immunocytochemistry

Immunohistochemistry of cells in culture was performed as follows: cells on glass coverslips were fixed in 3.7% formaldehyde for 10 minutes and permeabilized with 0.25% Triton X-100 for 10 minutes at room temperature (RT). Cells were then incubated with blocking solution (1× phosphate-buffered saline [PBS]/2% horse serum/5% bovine serum albumin) for 1 hour at RT, followed by incubation with primary antibodies for 1 hour at RT. Primary antibodies to cardiac markers were mouse monoclonal anti-tropomyosin I (MAB1691; 1:300; Millipore, Billerica, MA, <http://www.millipore.com>), sheep polyclonal anti-tropomyosin (ab5441; 1:300; Abcam, Cambridge, MA, <http://www.abcam.com>), and mouse monoclonal anti-actinin (MAB1682; 1:100; Millipore). Rabbit polyclonal anti-connexin 43 (C6219; 1:300; Sigma-Aldrich, St. Louis, MO, <http://www.sigmaaldrich.com>) was used for detecting gap junctions. Next, cells were washed with 1× PBS and incubated with secondary antibodies (Jackson ImmunoResearch Laboratories, West Grove, PA, <http://www.jacksonimmuno.com>) for 1 hour at RT, and then coverslips were mounted using Vectashield mounting medium including 4',6-diamidino-2-phenylindole (DAPI) (Vector Laboratories, Burlingame, CA, <http://www.vectorlabs.com>).

For immunohistochemistry of cardiac tissue, hearts were collected, weighed, frozen in liquid nitrogen-cooled 2-methylbutane, and stored at -80°C . Serial sections from frozen hearts were cut in 10- μm -thick slices and collected on numbered slides. Sections were fixed and blocked as listed above for cells on glass coverslips. Sections were incubated with primary antibody for 1 hour at RT except for Nestin and Ki67 antibody, which were incubated overnight at 4°C . Primary antibodies used were dystrophin (ab15277; 1:1,000; Abcam), CD31 (ab28364; 1:300; Abcam), DDR2 (sc-7555; 1:100; Santa Cruz Biotechnology Inc., Santa Cruz, CA, <http://www.scbt.com>), Ki67 (#550609; 1:300; BD Pharmingen, San Diego, CA, http://wwwbdbiosciences.com/index_us.shtml), Nestin (CH23001; 1:100; Neuromics, Edina, MN, <http://www.neuromics.com>), and cardiac troponin I (MAB3150; 1:100; Millipore).

Immunohistochemistry Data Analysis

For digital images, a Retiga 2000R digital camera (QImaging, Surrey, BC, Canada, <http://www.qimaging.com>) was used with a Leica (Heerbrugg, Switzerland, <http://www.leica.com>) inverted DMI 4000B microscope. Images were assigned color and merged using Image Pro Plus software (MediaCybernetics, Bethesda, MD, <http://www.mediacy.com>), which was also used for counting and measuring primary antibody-stained positive areas. Ten fields of view were taken randomly for quantitation of Ki67⁺, nestin⁺, and DDR2⁺ cells in the myocardium, CD31 area, and the numbers of DDR2⁺ and cardiac troponin I (cTnI)⁺ Dil-labeled cells. The field of view with the $\times 40$ objective measured $260 \times 225 \mu\text{m}$, and the field of view with a $\times 20$ objective measured $540 \times 450 \mu\text{m}$. For nestin- and DDR2-positive cells, data are given as number of cells expressing markers per field of view, using the $\times 40$ objective. Ki67⁺ cells are presented as the percentage of cells in each field of view with Ki67, using the $\times 20$ objective. The percentage of Ki67 cells was obtained by dividing the number of Ki67⁺ cells per field by the number of DAPI-labeled nuclei per that same field. CD31-positive area per field of

view was obtained with the $\times 20$ objective. For the percentage of Dil⁺ ADMs expressing DDR2 or cTnI, the number of Dil-labeled cells expressing these markers was divided by the total number of Dil-labeled cells.

Cardiac Specific Gene Expression by Reverse Transcription-Polymerase Chain Reaction

Expression of cardiac-specific transcription factors in ADMs after 14 days in differentiation medium was detected by reverse transcription-polymerase chain reaction (RT-PCR). The total RNA from cells grown as a monolayer was isolated by Trizol reagent (catalog no. 15596-018; Invitrogen, Carlsbad, CA, <http://www.invitrogen.com>), and cDNA was synthesized using a LongRange 2Step RT-PCR kit (catalog no. 205920; Qiagen, Hilden, Germany, <http://www.qiagen.com>) as per the manufacturers' instructions. The primers used in RT-PCR are listed in supplemental online Figure 5.

Generation of ADM Stable Green Fluorescence Protein Transfectants

For the preparation of green fluorescence protein (GFP)-labeled ADMs, the cells were maintained on gelatin-coated plates in proliferation medium. The cells were transfected with pRES2-AcGFP1 (Clontech, Palo Alto, CA, <http://www.clontech.com>) using Lipofectamine 2000 reagent (Invitrogen) according to the product instruction manual. After transfection the cells were cultured in proliferation medium with 400 mg/ml G418. The transfected cells were sorted by fluorescence-activated cell sorting using an iCyt automated imaging cytometer (Sony Biotechnology Inc., Champaign, IL, <http://www.i-cyt.com>) based on positive GFP signal. Nontransfected control cells were used to set the background fluorescence. GFP-positive cells were detected by using the 520 λ channel and sorted for purity at 2,000 cells per second. After sorting, GFP-positive cells were maintained in proliferation medium with 20 ng/ml LIF and 400 mg/ml G418.

ADM Labeling With Dil

ADMs were trypsinized, washed, and incubated with Dil (1,1'-diiododecyl-3,3,3'-tetramethylindocarbocyanine perchlorate) at a concentration of 1×10^6 cells per milliliter with 5 μl of Dil/ml in proliferation medium for 30 minutes in a humidified incubator at 37°C in 5% CO_2 prior to the transplantation. After being washed three times with Hanks' balanced saline solution (HBSS), Dil-labeled ADMs were resuspended in HBSS at 5×10^6 cells per 50 μl . For double labeling GFP-transfected ADMs were labeled with Dil prior to the transplantation using the same protocol.

Mice

All mice were handled according to a protocol approved by the University of Illinois Institutional Animal Care and Use Committee. *mdx/utrn*^{-/-} dystrophin- and utrophin-deficient mice are a phenotypic model for Duchenne muscular dystrophy; they develop progressive pathology in skeletal and cardiac muscle, ventricular dilation, and a resulting decrease in heart function [45, 46]. *mdx/utrn*^{-/-} mice were generated by interbreeding *mdx/utrn*^{+/-} mice [45], and the progeny were genotyped as previously described [48]. *mdx* mice were obtained using the same breeding scheme. Because the *mdx* and *utrn*^{-/-} mice used to generate the *mdx/utrn*^{+/-} mice were both maintained on a C57Bl background, we used C57Bl/10 mice for age-matched wild-type controls.

Cardiac Injection of ADMs

Labeled ADMs were transplanted into the wall of the left ventricle of mice as previously described [49, 50]. Briefly, mice were anesthetized by halothane (Halocarbon, River Edge, NJ, <http://www.halocarbon.com>) mixed in mineral oil (7.5 ml of halothane/40 ml of mineral oil), and Bactoshield CHG 4% solution (Steris, Mentor, OH, <http://www.steris.com>) was used to scrub the anterior chest area of mice. Insulin syringes (a 0.3-ml syringe with a 29-gauge needle) with 5×10^6 cells in 50 μ l of HBSS were injected into the fifth intercostal space to the left side of the sternum where the left ventricular wall is located. The plunger was slowly pushed, and the needle was retracted gently. Following injection of cells mice were placed on a heating pad, and their condition was observed until they were fully recovered.

mdx/utrn^{-/-} mice were injected with cells at 5–6 weeks of age, prior to the onset of pathology and dilated cardiomyopathy [44], and euthanized 5 weeks later. In our previous study we discovered greater regeneration, decreased degeneration, and more dystrophin in skeletal muscle of *mdx/utrn*^{-/-} mice 9 weeks postinjection in comparison with 5 weeks postinjection [37]. However, many mice did not survive 9 weeks following injection. We therefore chose to examine mice 5 weeks after transplantation for the current study. *mdx* mice were injected with GFP/Dil double-labeled ADMs at 5 weeks of age to determine whether cells survived and expressed cardiac markers. Later, to determine whether ADMs alleviated dilated cardiomyopathy, Dil-labeled ADMs were injected into the heart of aged *mdx* mice between 14 and 16 months of age. Because *mdx* mice commonly survive to 2 years of age, we chose to observe them 9–10 weeks following transplantation for analysis of heart function and histology.

Echocardiography

Two-dimensional M-mode echocardiography was used to measure heart function. A baseline echocardiograph was performed on 5-week-old *mdx/utrn*^{-/-} mice and 14–16-month-old *mdx* mice prior to cell transplantation. Echocardiography was performed once again 5 weeks after cell transplantation in *mdx/utrn*^{-/-} mice and 10 weeks after cell transplantation in *mdx* mice. GE/Vingmed ultrasound Vivid7 (GE Healthcare, Little Chalfont, U.K., <http://www.gehealthcare.com>) was used for performing echocardiographs with *mdx* mice, and Ultrasound-Visual Sonics Vevo 2100 (Visualsonics, Toronto, ON, Canada, <http://www.visualsonics.com>) was used for performing echocardiographs with *mdx/utrn*^{-/-} mice. Mice were anesthetized by halothane in mineral oil as described above. The chest hairs were clipped, ultrasound gel was placed on the transducer, the transducer was placed on top of the chest, and images were acquired. *mdx* and *mdx/utrn*^{-/-} mice were presented with age-matched wild-type mice randomly to the echocardiographer (R.O.), who was blinded to the genotype of mice.

Echocardiography Statistical Analysis

The Proc Mixed procedure of SAS (SAS Institute, Inc., Cary, NC, <http://www.sas.com>) was used to analyze the echocardiograph data. The statistical model included effects of genotype, ages, time point of performing echocardiographs, and their interaction as fixed effects. Differences between before and after cell transplantation within each genotype and among genotypes within each time point of performing echocardiography were

tested by pairwise comparisons when the main effects were significant.

RESULTS

Aorta-Derived Mesoangioblasts Express Cardiomyocyte Markers In Vitro

ADMs were induced to adopt a cardiomyocyte-like morphology by using commercially available cardiomyocyte medium, using a serum-free medium supplement, or adding 2% horse serum to medium. ADMs in proliferation medium have a spindle shape (Fig. 1A), as previously reported for clonally derived, undifferentiated mesoangioblasts [37, 47]. However, when ADMs were cultured in differentiation media, a morphology similar to control rat cardiomyocytes was observed, with a large, flat cytoplasm and tight contact with adjacent cells (Fig. 1B). At these points of contact, connexin 43 (Cx43), a gap junction protein important for electrical coupling of cardiomyocytes in the heart, was detected (Fig. 1C).

The change in morphology was gradual. At day 9 in differentiation medium, less than 40% of cells had cardiomyocyte-like morphology, but 97.82% of cells had cardiomyocyte-like morphology by day 14 (Fig. 1D). ADMs also expressed cardiac-specific mRNA and proteins in differentiation medium. Cardiac-specific homeobox transcription factor Nkx2.5, cardiac troponin I (cTnI), and cardiac tropomyosin (cTm) were detected in differentiated ADMs by RT-PCR (Fig. 1E). In addition cTnI, cTm, and α -actinin proteins were also detected by immunohistochemistry (Fig. 1F–1L). At day 14 in N2B27 differentiation medium, 69% of ADMs expressed cTm protein compared with 7% of ADMs in proliferation medium (Fig. 1F).

Aorta-Derived Mesoangioblasts Express Cardiomyocyte Markers After Transplantation Into Young *mdx* Heart

Undifferentiated ADMs were transplanted into cardiac muscle of 5-week-old *mdx* mice ($n = 2$). ADMs stably transfected with GFP (96.33% of cells) (Fig. 2A, 2B) were colabeled with the lipophilic dye Dil prior to injection and were detected in the ventricles of the heart immediately following injection (Fig. 2C–2F). ADMs were singly labeled with Dil for subsequent experiments, as ADMs silenced GFP expression over time, and GFP stable transfectants did not differentiate into some mature cell types in vivo (data not shown).

cTnI, a marker of cardiomyocytes, was detected in Dil-labeled cells in the heart 6 weeks following injection of Dil-labeled ADMs (Fig. 2G–2J). Dil and dystrophin protein colocalization was also observed in the ventricles of *mdx* heart after ADM transplantation (Fig. 2K, 2L). However, dystrophin was detected only in limited regions of the heart rather than throughout the entire ventricle.

ADM Transplantation Prevents Ventricular Dilation and Decreased Heart Function in *mdx/utrn*^{-/-} Cardiac Muscle

Cardiac ultrasound was used to assess heart function and ventricular dilation before and after ADM transplantation. *mdx/utrn*^{-/-} mice were injected with either ADMs or an equal volume of saline solution as a control at approximately 5–6 weeks of age. Age-matched wild-type mice were also injected with saline solution as a control. Neither age-matched wild-type

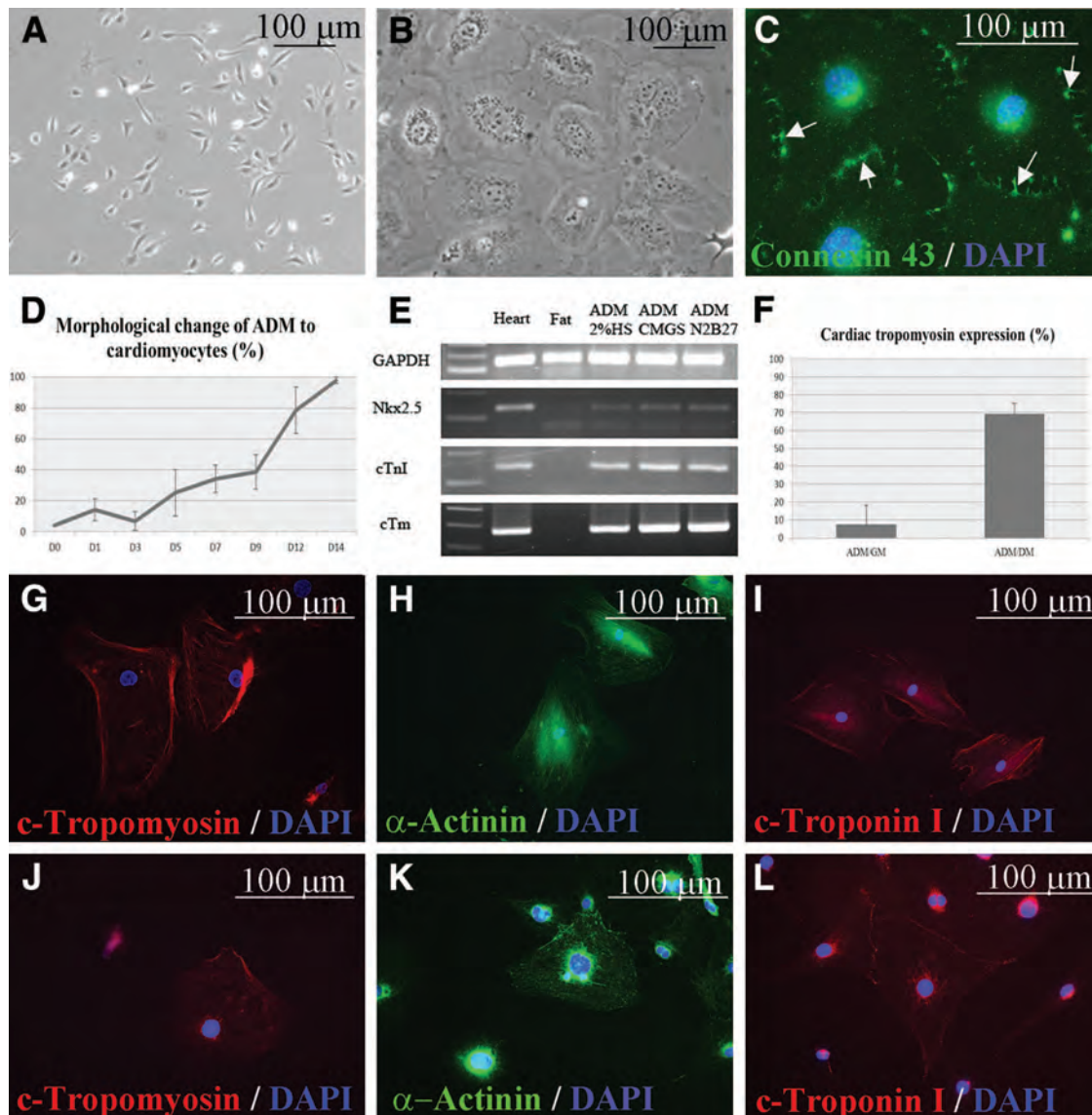


Figure 1. ADMs adopt cardiomyocyte-like morphology and express cardiac markers in vitro. ADMs were differentiated into cardiac myocytes in vitro, and expression of cardiac-specific genes and proteins was evaluated. **(A, B)**: Morphology of ADMs in growth medium **(A)** and cardiac differentiation medium **(B)**. **(C, D)**: ADMs in differentiation medium expressed connexin 43 in regions where adjacent cells met (white arrows) **(C)** and adopted a cardiomyocyte morphology slowly over time **(D)**. **(E)**: ADMs in differentiation medium expressed cardiac-specific mRNA, including *Nkx2.5*, *cTnI*, and *cTm*. Heart tissue was used as a positive control and adipose as a negative control for cardiac markers. GAPDH was used as an internal loading control. **(F–L)**: ADMs expressed cardiac proteins in differentiation medium, including cardiac *cTm* **(J)**, α -actinin **(K)**, and *cTnI* **(L)**. Primary rat cardiomyocytes were used as a positive control for cardiac proteins **(G–I)**. **(F)**: Quantitation of cells expressing *cTm*. Blue in **(C, G–L)** indicates DAPI-stained nuclei. Abbreviations: ADM, aorta-derived mesoangioblast; CMGS, cardiomyocyte growth supplement; *cTm*, cardiac tropomyosin; *cTnI*, cardiac troponin I; DAPI, 4',6-diamidino-2-phenylindole; DM, differentiation medium; GAPDH, glyceraldehyde-3-phosphate dehydrogenase; GM, growth medium; HS, horse serum.

mice injected with saline solution nor *mdx/utrn*^{-/-} mice injected with ADMs demonstrated significant changes in the thickness of the heart wall or septum, ventricular dilation, or a decrease in heart function, as measured by ejection fraction (EF), end diastolic volume (EDV), and fractional shortening (FS) by 10–11 weeks of age (Fig. 3A–3D; raw data available in supplemental online Fig. 1; wild-type mice injected with saline, *n* = 4; *mdx/utrn*^{-/-} mice injected with saline, *n* = 4; *mdx/utrn*^{-/-} mice injected with ADMs, *n* = 5). In contrast, statistically significant decreases in the thickness of the left ventricular wall (Fig. 3A) and an increase in the diameter of the left ventricle at both diastole and systole (Fig. 3B; supplemental online Fig. 1), as

well as a large increase in EDV (Fig. 3C), were observed in *mdx/utrn*^{-/-} mice injected with saline solution (Fig. 3A–3D), consistent with development of dilated cardiomyopathy. Baseline values in EDV and left ventricular internal dimension, prior to injection, differed between groups of animals but correlated with the weight of the groups of animals at the time of stem cell injection (Fig. 3E), consistent with a previous report demonstrating a linear relationship between body weight and these ultrasound parameters in a variety of different species [51]. The heart weight/body weight ratio of mice was not significantly different between groups at the time of euthanasia (Fig. 3F).

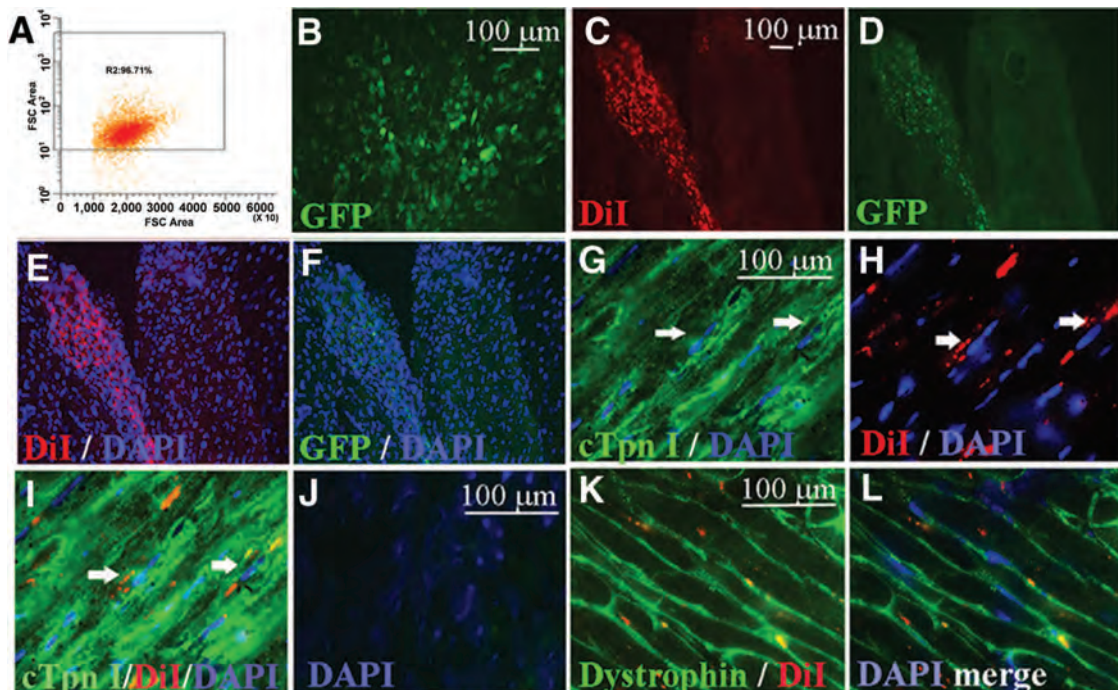


Figure 2. Aorta-derived mesoangioblast (ADM) labeling, transplantation, and cardiac marker expression in the heart. ADMs were labeled and transplanted into the heart of *mdx* mice, and fluorescent microscopy was used to detect the expression of cardiac-specific proteins in ADMs following transplantation. (**A, B**): ADMs were stably transfected with pIRES2-AcGFP1 and selected for GFP expression intensity using fluorescence-activated cell sorting. (**C–F**): GFP-transfected ADMs (green [**D, F**]) were colabeled with Dil (red [**C, E**]) and injected into the heart wall in 5-week-old *mdx* mice. Dual-labeled GFP+ Dil+ cells were detected in the ventricles of the heart 5 weeks later. (**G–J**): Dil (red, [**H, I, K, L**]) was detected in cells expressing cardiac troponin I protein (green [**G, I**]), and dystrophin (green [**K, L**]) in the myocardium of the ventricles. (**J**): Tissue incubated with secondary, FITC-conjugated antibody only. Blue in (**E–J, L**) indicates DAPI-stained nuclei. Abbreviations: cTpn I, cardiac troponin I; DAPI, 4',6-diamidino-2-phenylindole; FITC, fluorescein isothiocyanate; FSC, forward scatter; GFP, green fluorescence protein.

ADM Injection Results in Dystrophin Expression and an Increase in CD31 Expression in *mdx/utrn*^{-/-} Heart After ADM Injection

Dystrophin expression (Fig. 4A, 4B, wild-type cardiac muscle) was detected in ADM-injected (Fig. 4C, 4D) but not saline-injected *mdx/utrn*^{-/-} heart (Fig. 4E, 4F) or ADM-injected *mdx* heart (Fig. 4G, 4H, discussed in more detail below). Because functional benefit from transplantation of exogenous stem cells frequently results from indirect effects, including angiogenesis [52], we examined expression of the endothelial cell marker CD31 (Fig. 4I, 4J). CD31 expression was significantly higher in *mdx/utrn*^{-/-} heart injected with ADMs compared with *mdx/utrn*^{-/-} mice injected with saline or age-matched sham-injected wild-type control mice (Fig. 4K). No significant difference in CD31 expression was observed between wild-type control mice or *mdx/utrn*^{-/-} mice injected with saline (Fig. 4K).

ADM Injection Normalizes Numbers of Nestin⁺ Interstitial Dividing Cells and Correlates With the Appearance of Nestin⁺ Striated Cells in the Heart of *mdx/utrn*^{-/-} Mice

To assess whether the ADMs prevent DCM by stimulating endogenous cardiac stem cells to divide for repair and regeneration of the heart, we examined cell proliferation in the heart. The adult heart is largely postmitotic, but it contains a population of dividing cardiac progenitor cells that expand following damage and are thought to contribute to homeostasis [53]. In wild-type adult heart, as expected, numerous Ki67⁺ cells were detected

in the ventricles of the heart (Fig. 5A, 5B, 5G–5J; *n* = 4). Unexpectedly, there were approximately fivefold fewer proliferating endogenous cells in *mdx/utrn*^{-/-} heart injected with saline solution (Fig. 5C, 5D, 5J; *n* = 4). However, ADM injection normalized numbers of proliferating cells in *mdx/utrn*^{-/-} heart (Fig. 5E, 5F, 5J; *n* = 5). Ki67⁺ cells in the myocardium did not express Sca-1, a marker on many resident cardiac stem cells, but did express nestin (Fig. 5K, 5L), a marker present on neural-crest-derived stem cells in normal and infarcted myocardium [54–57]. Despite the increase in proliferating nestin⁺ cells in ADM-injected *mdx/utrn*^{-/-} myocardium, there were significantly fewer total numbers of nestin⁺ cells in the interstitium of ADM-injected myocardium (Fig. 6A). While quantitating nestin⁺ interstitial cells in the myocardium of the ADM- or sham-injected mice, we observed nestin⁺ striated cells that expressed cardiac troponin I in the heart of four of five *mdx/utrn*^{-/-} mice injected with ADMs (Fig. 6B–6F). A small number were also observed in one of four hearts from an *mdx/utrn*^{-/-} mouse injected with saline (Fig. 6G), but nestin⁺ striated cells were not present in myocardium from age-matched wild-type sham-injected mice (Fig. 6H, *n* = 4).

Fate of ADMs Following Transplantation Into *mdx/utrn*^{-/-} Heart

Few Dil-labeled cells were detected in the myocardial layer of *mdx/utrn*^{-/-} hearts 5 weeks following injection, despite the observation that dystrophin-positive cardiomyocytes were present. Dil cells were detected in the epicardium, of which approximately half ($54.94 \pm 9.23\%$) expressed the cardiac fibroblast

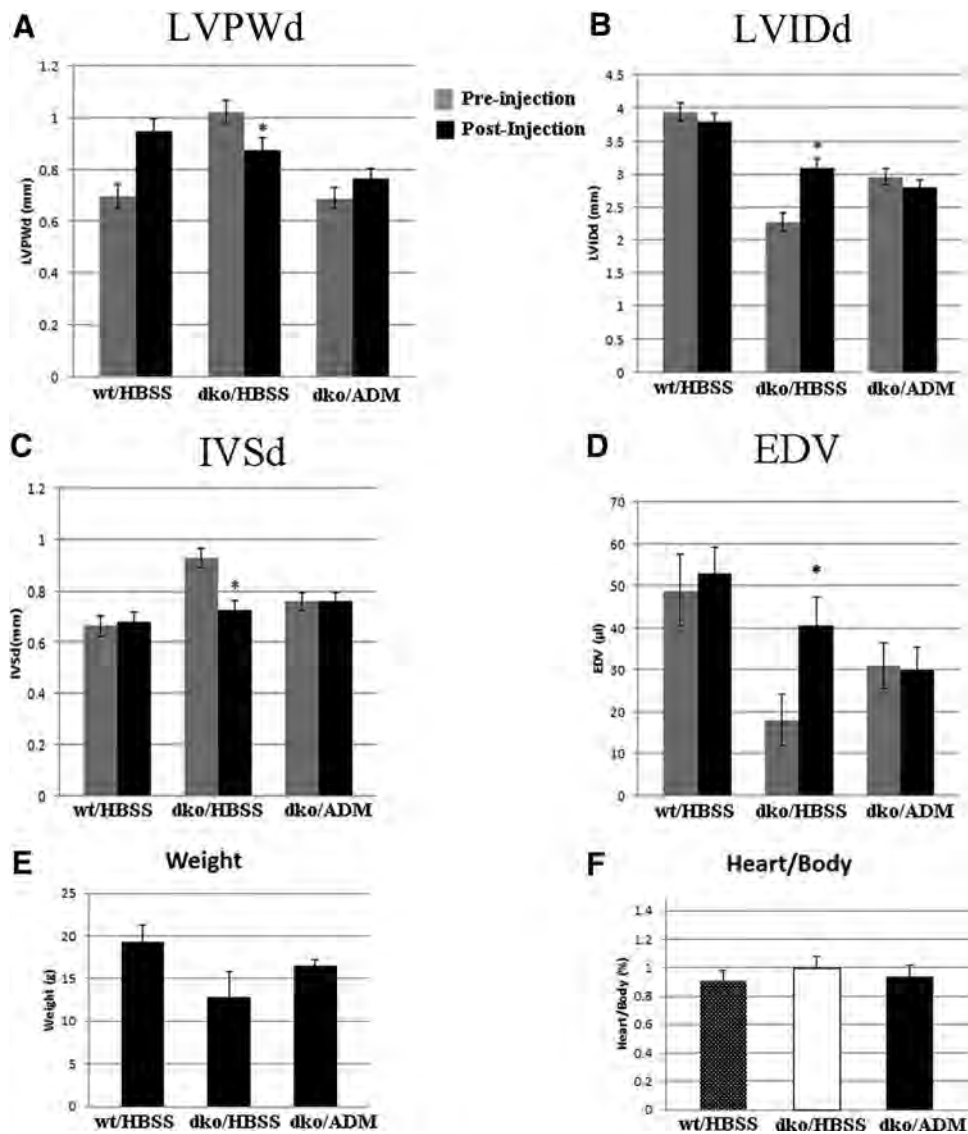


Figure 3. ADMs transplanted into *mdx/utrn*^{-/-} heart delays onset of dilated cardiomyopathy. Control and *mdx/utrn*^{-/-} mice received intracardiac injections of saline or ADMs, and heart function, ventricle size, and heart wall thickness were measured using cardiac ultrasound. (A–C): *mdx/utrn*^{-/-} control mice injected with saline (dko/HBSS; *n* = 4) exhibited a significant thinning of the LVPWd (A), increase in the LVIDd (B), and thinning of the internal ventricular septum (C), whereas age-matched wild-type mice (wt/HBSS; *n* = 4) and *mdx/utrn*^{-/-} mice injected with ADMs (dko/ADM; *n* = 5) did not. (D): A large increase in EDV was also observed in *mdx/utrn*^{-/-} mice injected with saline, but not in age-matched wild-type mice injected with saline or *mdx/utrn*^{-/-} mice injected with ADMs. (A–D): Gray bars, preinjection values; black bars, postinjection values. (E): Differing body weights among mice in the different treatment groups at the time of injection of ADMs or saline. (F): The heart-weight and body-weight ratio of mice in all groups was not different at the time of the last cardiac ultrasound and subsequent euthanasia. *, *p* < .05. Abbreviations: ADM, aorta-derived mesoangioblast; dko, double knockout *mdx/utrn*^{-/-}; EDV, end diastolic volume; HBSS, Hanks' balanced saline solution; IVSd, internal ventricular septum at diastole; LVIDd, left ventricular internal dimension at diastole; LVPWd, left ventricular posterior wall at diastole; wt, wild-type.

marker DDR2 and $17.93 \pm 2.98\%$ expressed cardiac troponin I (supplemental online Fig. 2). Dil-labeled cells in the myocardium are therefore likely committed to becoming cardiac fibroblasts or cardiomyocytes.

ADM Injection Does Not Prevent Changes Associated With Dilated Cardiomyopathy in Aged *mdx* Mice

To assess whether ADMs alleviate existing cardiomyopathy, we transplanted cells into the hearts of aged 12–14-month-old *mdx* mice and performed cardiac ultrasound before and 10 weeks after injection. Ventricular dilation and wall thinning were not present in *mdx* mice at the time of the initial echo (Fig. 7A, 7B,

wild-type mice injected with saline, *n* = 3; *mdx* mice injected with saline, *n* = 4; *mdx* mice injected with ADMs, *n* = 4). However, following stem cell injection, *mdx* mice exhibited changes consistent with the development of dilated cardiomyopathy (Fig. 7; supplemental online Fig. 3). Both sham- and ADM-injected *mdx* mice exhibited significant ventricular dilation 10 weeks after injection, in comparison with wild-type mice (Fig. 7A). However, the greatest degree of change following injection was observed in *mdx* heart injected with ADMs, in which a large increase in ventricular dilation was present following cell transplantation (Fig. 7A). Wall thinning was observed in *mdx* heart following saline injection (Fig. 7B), consistent with early ventricular

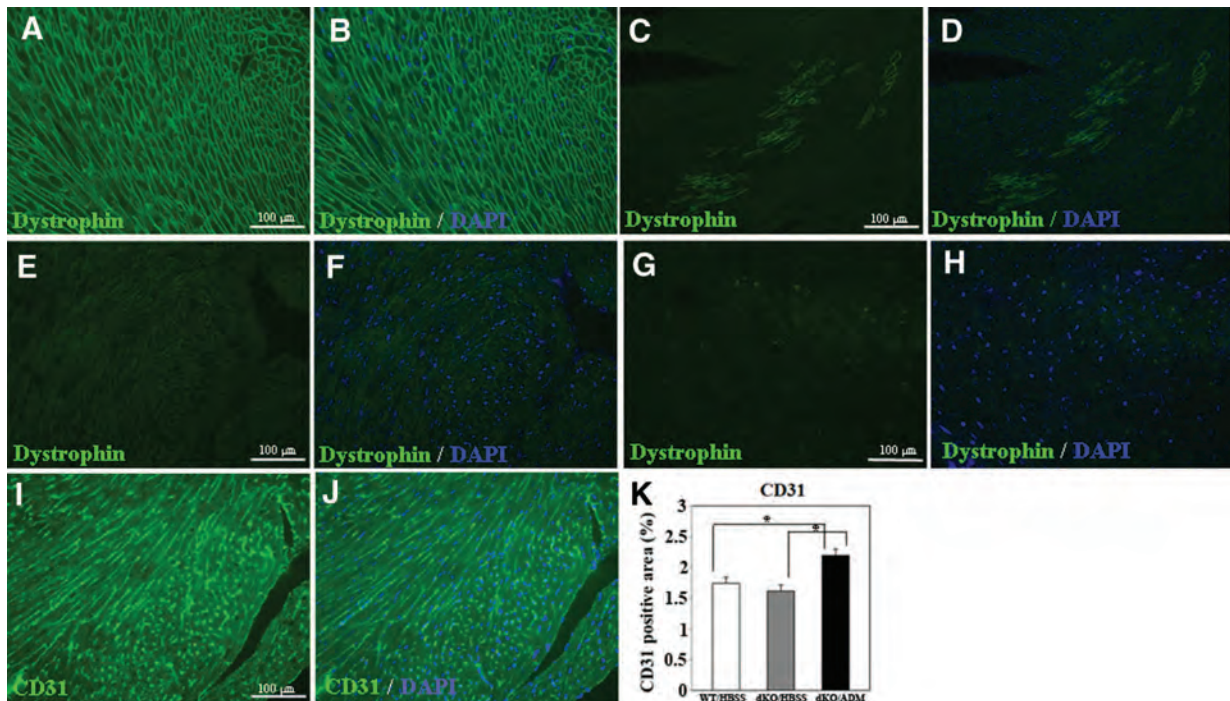


Figure 4. Dystrophin expression and angiogenesis are detected in cardiac muscle of *mdx/utrn*^{-/-} mice injected with ADMs. Fluorescent microscopy was used to analyze the expression of dystrophin and CD31 in the hearts of wild-type, *mdx/utrn*^{-/-}, and *mdx* mice following transplantation of cells or saline injection. (A, B): Wild-type control mice with saline injection were used as a positive control for dystrophin protein expression (green). (C, D): Dystrophin was detected in some cells in the myocardium of *mdx/utrn*^{-/-} mice following ADM injection (*n* = 5). (E, F): No dystrophin was detected in *mdx/utrn*^{-/-} mice injected with saline (*n* = 4). (G, H): Dystrophin was not detected in the myocardium of *mdx* mice after ADM injection (*n* = 4). (I–K): CD31 (green), a marker of endothelial cells, was detected by immunofluorescent microscopy and quantified in all groups of mice. (A, C, E, G): Dystrophin (green). (B, D, F, H): Merged images of dystrophin (green) and DAPI (blue). (I, J): Representative image of CD31 in wild-type control myocardium. (K): Quantitative analysis of CD31 expression revealed higher CD31 expression in *mdx/utrn*^{-/-} myocardium injected with ADMs (dKO/ADM; *n* = 5) than in *mdx/utrn*^{-/-} myocardium injected with saline (dKO/HBSS; *n* = 4) or in age-matched wild-type mice injected with saline solution (WT/HBSS; *n* = 4). *, statistically significant difference (*p* < .05) between the groups indicated. Abbreviations: ADM, aorta-derived mesoangioblast; DAPI, 4',6-diamidino-2-phenylindole; dKO, double knockout *mdx/utrn*^{-/-}; HBSS, Hanks' balanced saline solution; WT, wild-type.

remodeling [58, 59]. *mdx* mice injected with ADMs had a thicker ventricular wall following transplantation (Fig. 7B; supplemental online Fig. 3), consistent with later stages of ventricular remodeling following damage [58–59]. *mdx* mice injected with saline or with ADMs exhibited a significant decline in heart function, measured by EF and FS, in contrast to age-matched wild-type mice, which did not demonstrate declining heart function after saline injection (Fig. 7C, 7D). Other measures of heart function, EDV and end systolic volume (ESV), did not change in wild-type heart or *mdx* heart after sham injection and were also not different between control wild-type and *mdx* mice (supplemental online Fig. 3). However, a dramatic increase in both EDV and ESV was observed in *mdx* heart injected with ADMs (Fig. 7E; supplemental online Fig. 3), also consistent with the later stages of ventricular remodeling following damage and with poorer survival following recovery from damage [58–60].

Dystrophin, Angiogenesis, and Stem Cell Proliferation Are Not Present Following ADM Injection Into Aged *mdx* Heart

In contrast to the hearts of *mdx/utrn*^{-/-} mice (Fig. 4C, 4D; *n* = 5) and young *mdx* mice (Fig. 2K, 2L, *n* = 2) injected with ADMs, dystrophin was not detected in aged *mdx* hearts injected with ADMs (Fig. 4G, 4H, *n* = 4). Consistent with cardiac ultrasound data indicating ventricular remodeling in *mdx* mice, fibrosis was present in the hearts of both groups of *mdx* mice but not in

age-matched wild-type hearts (Fig. 7F). In contrast to the increase in CD31 observed with ADM transplantation in *mdx/utrn*^{-/-} hearts, there was no difference in CD31 with ADM transplantation into aged *mdx* heart, or between aged *mdx* and wild-type heart (Fig. 7G). Similar to *mdx/utrn*^{-/-} mice (Fig. 5G), there was a significant decrease in the number of endogenous dividing cells in *mdx* heart (Fig. 7H), but ADM injection did not normalize this in *mdx* mice (Fig. 7H).

DISCUSSION

In this study we tested whether ADMs prevent or alleviate dilated cardiomyopathy in murine models for DMD. ADMs are derived from newborn or juvenile postnatal aorta and have a marker profile similar to that of mesoangioblasts derived from embryonic dorsal aorta and postnatal ventricle [47, 61–63]. Injection of ADMs into the hearts of *mdx/utrn*^{-/-} mice prior to the onset of disease prevented thinning of the left ventricular wall and chamber dilation, as well as an increase in EDV, observed in control, sham-injected *mdx/utrn*^{-/-} mice (Fig. 3). Postinjection echo parameters were not significantly different between age-matched *mdx/utrn*^{-/-} mice and wild-type mice at 10–11 weeks of age, even with highly significant changes in the hearts of sham-treated *mdx/utrn*^{-/-} mice (Fig. 3; supplemental online Fig. 1). For example, although highly significant ventricular dilation was observed in the control *mdx/utrn*^{-/-} mice over time

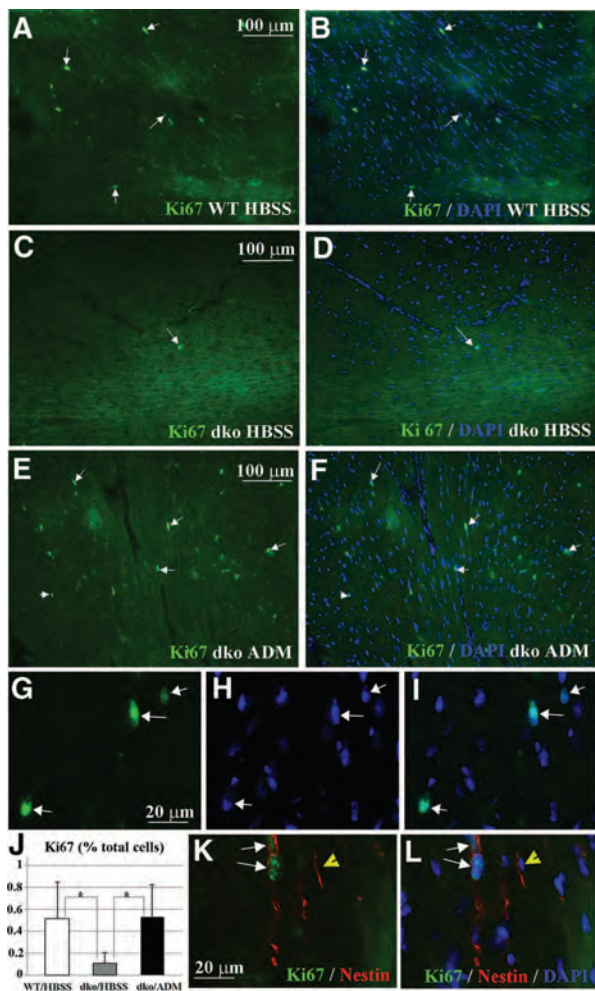


Figure 5. Basal levels of dividing cells are maintained in aorta-derived mesoangioblast (ADM)-transplanted *mdx/utrn*^{-/-} myocardium. Ki67 expression was analyzed to determine the percentage of dividing cells in heart tissue from wild-type and *mdx/utrn*^{-/-} mice injected with ADMs or saline. Ki67, a marker for dividing cells, was detected with immunofluorescent microscopy in nuclei in the heart of wild-type mice injected with saline injection (WT/HBSS; *n* = 4) (A, B), *mdx/utrn*^{-/-} mice with saline injection (dKO/HBSS; *n* = 4) (C, D), and *mdx/utrn*^{-/-} mice with ADM injection (dKO/ADM, *n* = 5) (E, F). White arrows indicate Ki67⁺ nuclei (A–I, K, L) that colocalized with DAPI (B, D, F, I, L). (G–I): High-magnification images of heart tissue from wild-type mice injected with saline, with Ki67⁺ nuclei (green [G]) that colocalized with DAPI (blue [H, I]). Ki67-positive cells were quantified in images captured using the magnification in (G–I). (J): There were significantly fewer dividing cells in the myocardium of sham-injected *mdx/utrn*^{-/-} mice (gray bar) compared with age-matched control wild-type mice (white bar). However, ADM-injected *mdx/utrn*^{-/-} myocardium had significantly higher numbers of dividing cells (black bar) than saline-injected *mdx/utrn*^{-/-} myocardium. The numbers of dividing cells in ADM-injected *mdx/utrn*^{-/-} heart were not significantly different from the basal levels observed in wild-type myocardium. *p* values were obtained using Student's *t* test. An antibody to the neural stem and progenitor marker nestin was used to determine whether the Ki67⁺ dividing cells expressed nestin. (K, L): Ki67⁺ nuclei (green) were detected in cells expressing nestin (red). White arrows indicate nestin⁺ cells that are dividing and have nuclear Ki67⁺ expression. The yellow arrowhead indicates a nestin⁺ cell that is not proliferating and does not express Ki67. (L): Merged image from (K) with DAPI. (B, D, F, I, L): Merged images of Ki-67, or Ki-67 and nestin (L) with DAPI (blue). (J): *, statistically significant difference between the groups indicated (*p* < .05). Abbreviations: DAPI, 4',6-diamidino-2-phenylindole; dko, double knockout *mdx/utrn*^{-/-}; HBSS, Hanks' balanced saline solution; WT, wild-type.

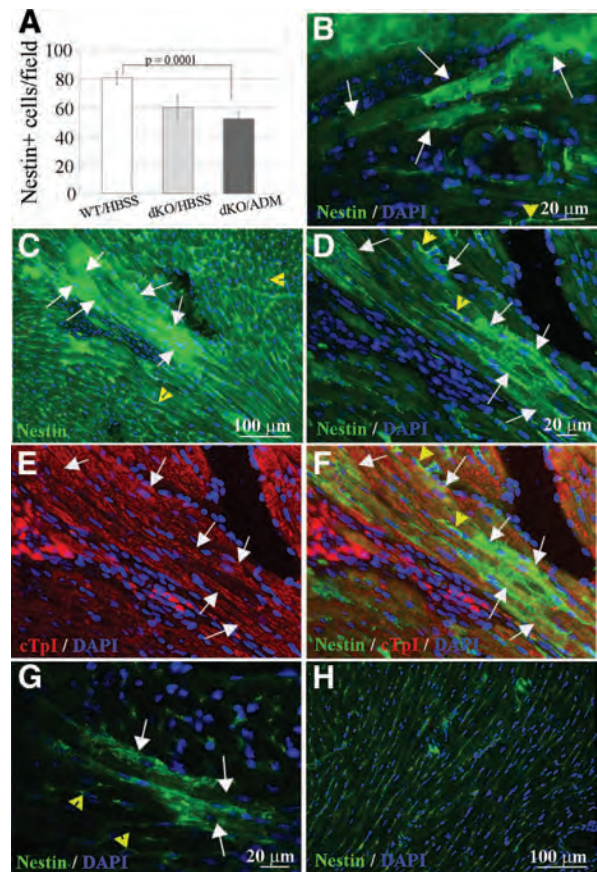


Figure 6. Nestin⁺ interstitial stem cells and cardiac myocytes in ADM-transplanted *mdx/utrn*^{-/-} heart. Fluorescent microscopy was used to visualize nestin⁺ interstitial and striated cells in the heart. (A): There were significantly fewer nestin⁺ interstitial stem cells in ADM-injected (dKO/ADM, *n* = 5) *mdx/utrn*^{-/-} heart in comparison with age-matched wild-type heart injected with saline (WT/HBSS, *n* = 4). *p* values were obtained using Student's *t* test. No difference was observed between WT/HBSS versus dKO/HBSS (*p* = .0538) or dKO/HBSS versus dKO/ADM (*p* = .3843). (B–F): Nestin⁺ striated cells (green, indicated by white arrows) were observed in four of five *mdx/utrn*^{-/-} hearts transplanted with ADMs. (C): A cluster of nestin⁺ striated cells (green, indicated by white arrows) and surrounding tissue containing nestin⁺ interstitial stem cells (also green, indicated by yellow arrowheads). (D–F): The same cluster of nestin⁺ cells (green) shown in (C), at higher magnification, expressed cardiac troponin I (red [E, F]). (G): Some nestin⁺ striated cells were also observed in one of four *mdx/utrn*^{-/-} hearts injected with saline. (H): Nestin⁺ striated cells were not present in saline-injected wild-type heart. Abbreviations: ADM, aorta-derived mesoangioblast; cTnI, cardiac troponin I; DAPI, 4',6-diamidino-2-phenylindole; dKO, double knockout *mdx/utrn*^{-/-}; HBSS, Hanks' balanced saline solution; WT, wild-type.

(*p* < .0001), the ventricles were still smaller than those of wild-type control mice at the time of the final echo at 11 weeks of age. These changes are related to the difference in body weight between the wild-type mice and the *mdx/utrn*^{-/-} mice, as wild-type mice are larger and therefore have larger ventricles than the *mdx/utrn*^{-/-} mice, as well as weight-related differences in other ultrasound parameters.

This is the first report of stem cell therapy yielding functional benefit in the dystrophin-deficient heart. Our data suggest multiple mechanisms by which ADMs prevent or delay the onset of dilated cardiomyopathy, including (a) differentiation or fusion

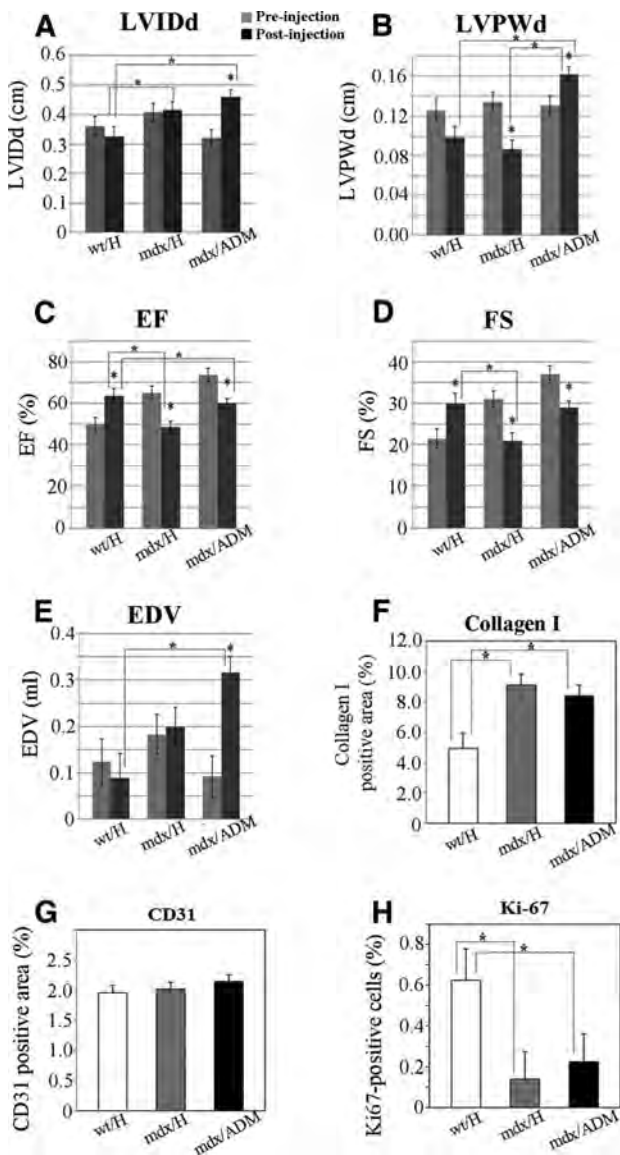


Figure 7. ADM transplantation into *mdx* myocardium does not alleviate symptoms of dilated cardiomyopathy or promote angiogenesis, dystrophin expression, or normalization of nestin⁺ cell division. Cardiac ultrasound was used to assess heart function, ventricular dilation, and thickness of the heart wall of wild-type or *mdx* mice transplanted with ADMs or saline. **(A):** Significant ventricular dilation was observed in both groups of *mdx* mice following injection of cells or saline compared with wild-type mice receiving sham (saline) injection ($n = 3$). *mdx* mice injected with ADMs also exhibited a significant increase in ventricular dilation after stem cell injection in comparison with preinjection values (denoted by asterisk over the postinjection bar). **(B):** *mdx* mice injected with saline solution ($n = 4$) exhibited significant thinning of the left ventricular wall between pre- and postinjection, whereas *mdx* mice injected with ADMs ($n = 4$) demonstrated a significant increase in the thickness of the ventricular wall between pre- and postinjection. The increase in thickness of the ventricular wall in ADM-transplanted *mdx* mice was significantly higher than that of both wild-type and *mdx* mice receiving sham injection. **(C, D):** *mdx* mice receiving either sham or ADMs suffered a significant decline in heart function after injection, measured by EF **(C)** and FS **(D)**. **(E):** EDV was significantly upregulated in *mdx* mice following ADM transplantation. Immunofluorescent microscopy was used to assess collagen I levels and expression of CD31 and Ki67 in wild-type or *mdx* mice injected with saline or ADMs. **(F):** Quantitative analysis of immunofluorescent staining for collagen,

with host cells to generate dystrophin-expressing cardiomyocytes, (b) induction of angiogenesis, and (c) stimulation of cell division and potentially cardiac differentiation of endogenous nestin⁺ neural stem cells in the heart. These data indicate that transplantation of ADMs may have clinical benefit, both direct and indirect, and a recent study reporting success in generating induced pluripotent stem-derived mesoangioblasts supports the feasibility of obtaining sufficient numbers of patient-specific mesoangioblasts for clinical use [64]. Generation of patient-specific mesoangioblasts would also allow for genetic correction and transplantation of autologous cells, decreasing the risk for immune response to donor cells. Dil-labeled ADMs were rarely observed in the myocardium of aged *mdx* mice or *mdx/utrn*^{-/-} mice. The low numbers of Dil⁺ donor cells observed could be due to ADM division within the heart following injection, resulting in dilution of Dil and/or to ADM cell death in vivo. The presence of dystrophin-positive cardiomyocytes suggests that some donor ADMs differentiate into cardiomyocytes or fuse with host cardiomyocytes, but dystrophin-positive cardiomyocytes were rare. Dil⁺ cells were detected in the epicardium and expressed DDR2 ($54.94 \pm 9.23\%$) and cTnI ($17.39 \pm 2.98\%$) but did not exhibit striations or morphology typical of mature cardiomyocytes (supplemental online Fig. 4).

Functional benefit following ADM injection may also be due, in part, to the increase in vasculature in the heart of *mdx/utrn*^{-/-} mice (Fig. 4I–4K). Angiogenesis is a well-known indirect effect of stem cell therapy for ischemic damage that results in improvements in heart function [52, 65–67]. Dystrophin-deficient dilated cardiomyopathy is not ischemic in origin, but there are data suggesting that ischemia may be present in DMD patients and murine models for DMD [68–72]. Abnormalities in small vessels including swollen endothelial cells and thickened basement membranes, conditions that may result in ischemia, have been observed in human patients [68–69], and vascular endothelial growth factor, known to be induced in ischemic conditions, is elevated in serum of DMD patients. Angiogenesis in dystrophin-deficient heart may therefore alleviate regions of ischemia to provide function benefit.

The increase in vasculature in dystrophin-deficient muscle may also have secondary beneficial effects by stimulating muscle regeneration. Induction of angiogenesis in dystrophin-deficient skeletal muscle has therapeutic benefit resulting from increased

with a statistically significant increase in collagen content of aged *mdx* heart in comparison with heart from age-matched wild-type mice. **(G):** There was no difference in CD31 expression in the myocardium between control and ADM-injected mice. **(H):** There was a significant decrease in resident dividing cells in *mdx* myocardium in comparison with age-matched wild-type myocardium, and ADM injection did not influence this number. **(A–E):** Gray bars, preinjection values; black bars, postinjection ultrasound values. **(F–H):** White bars, wild-type mice injected with saline; gray bars, *mdx* mice injected with saline; black bars, *mdx* mice injected with ADMs. WT/H: wild-type mice with saline injection ($n = 3$); mdx/H: *mdx* mice with saline injection ($n = 4$); mdx/ADM: *mdx* mice with ADM injection ($n = 4$). *, significant difference ($p < .05$) between the groups indicated. (An asterisk over the postinjection bar indicates a significant difference between pre- and postinjection values within a group of mice, whereas significant differences between groups of mice are indicated by lines between the two groups and an asterisk.) Abbreviations: ADM, aorta-derived mesoangioblast; EDV, end diastolic volume; EF, ejection fraction; FS, fractional shortening; H, saline injection; LVIDd, left ventricular internal dimension at diastole; LVPWd, left ventricular posterior wall at diastole; wt, wild-type.

numbers of muscle satellite cells and muscle fiber regeneration [73]. Many growth factors, cytokines, and chemokines are up-regulated in serum of DMD patients and *mdx* mice [74–78]. Increased exposure to those factors, through angiogenesis, may lead to the increase in nestin⁺ cell proliferation observed in our study. Nestin is expressed during heart development [79] and in a dormant state in the postnatal heart [80]. Nestin⁺ stem cells are also present in infarcted rat myocardium [54, 55], as well as in the infarct border zone in human patients with end-stage heart failure [56, 81], where they contribute to neuronal innervation, remodeling, and angiogenesis and give rise to Nkx2.5-positive cardiomyocytes after ischemic injury [56, 57, 81]. We have discovered that nestin⁺ cells proliferate in wild-type myocardium and that there is a significant decline in proliferation with dystrophin deficiency, which may result in a decreased ability to participate in innervation, angiogenesis, and formation of new cardiac muscle cells following damage. This would be consistent with the reported decline in proliferative potential of endogenous myogenic stem cells in skeletal muscle of DMD patients [82, 83] and decreased numbers of mesoangioblasts in patients with limb-girdle muscular dystrophy 2D [64]. Decreases in numbers of endogenous muscle stem cells have also been reported in animal models of muscular dystrophy. Kudryashova et al. recently reported decreased numbers, early senescence, and a decreased propensity for myogenic differentiation of activated endogenous satellite cells in skeletal muscle in a murine model for limb-girdle muscular dystrophy [84]. A recent report by Cassano et al. demonstrates that endogenous cardiac stem cells may also be affected [85]. The authors reported cardiac progenitor cells isolated from the heart of the golden retriever model for Duchenne muscular dystrophy are impaired in their ability to proliferate, self-renew, differentiate into cardiomyocytes in vitro, and undergo early senescence [85]. The decreased numbers and ability of stem cells to regenerate muscle have been shown to contribute to disease progression in skeletal muscle of *mdx* mice [86] and may also be responsible for cardiac remodeling in dystrophin-deficient heart. The decrease in nestin⁺ cells that we have observed in the *mdx* and *mdx/utrn*^{-/-} heart may translate into decreased regeneration following contraction-induced damage. ADM injection normalized numbers of nestin⁺ dividing cells, and we observed nestin⁺ striated cells that expressed cardiac troponin I in four of five *mdx/utrn*^{-/-} mice injected with ADMs. This is the first report of nestin⁺ striated cells in dystrophin-deficient heart and in response to nonischemic damage, and it indicates that they may be involved in the delay in DCM observed with ADM injection.

In contrast to *mdx/utrn*^{-/-} mice, injection of stem cells into the heart of 14–16-month-old *mdx* mice with existing cardiac pathology does not provide functional benefit, and in fact exacerbates some

characteristics of dilated cardiomyopathy. In addition to not observing functional benefit from ADM injection, we did not observe angiogenesis, dystrophin expression, or an increase in nestin⁺ stem cell division in the heart of aged *mdx* heart injected with ADMs. These differences may be due, in part, to the difference in utrophin status of the *mdx* and *mdx/utrn*^{-/-} mice. However, dystrophin expression is detected following injection of ADMs into the heart of young, 5-week-old *mdx* mice (Fig. 2K, 2L), suggesting that the differences observed following ADM injection may be related to the age of the mice and/or presence of pathology rather than to utrophin status. Therefore, the cardiac microenvironment may play a role in donor cell fate. In particular, fibrosis may inhibit ADM migration and survival, and integration with the myocardium. Fibrosis and scar tissue have also been shown to promote differentiation of exogenous stem cells into fibroblasts in scar tissue [87]. We did not observe an increase in the numbers of DDR2⁺ cardiac fibroblasts with ADM transplantation, indicating that ADMs do not contribute significantly to cardiac fibroblasts in the aged *mdx* heart (supplemental online Fig. 4).

CONCLUSION

Transplantation of wild-type ADMs with a functional copy of the dystrophin gene into dystrophin-deficient heart prevents dilated cardiomyopathy, inducing angiogenesis and proliferation of endogenous nestin⁺ stem cells in the heart, and correlates with nestin⁺ striated cells in the heart. However, timing of ADM transplantation is critical, as these events do not occur following injection into aged dystrophin-deficient heart where pathology is present.

ACKNOWLEDGMENTS

This work was supported in part by funds from the Illinois Regenerative Medicine Institute. M.H.S. is currently affiliated with the Department of Animal Science and Biotechnology, Chungnam National University, Daejeon, South Korea.

AUTHOR CONTRIBUTIONS

J.L.C., conception and design, collection and assembly of data, data analysis and interpretation, manuscript writing; R.O., collection of data, interpretation of data; M.H.S. and B.F.W., data analysis; S.E.B., conception and design, financial support, collection and assembly of data, data analysis and interpretation, manuscript writing, final approval of manuscript.

DISCLOSURE OF POTENTIAL CONFLICTS OF INTEREST

The authors indicate no potential conflicts of interest.

REFERENCES

- Emery AE. Population frequencies of inherited neuromuscular diseases: A world survey. *Neuromuscul Disord* 1991;1:19–29.
- Spurney CF, Gueron AD, Yu Q et al. Membrane sealant Poloxamer P188 protects against isoproterenol induced cardiomyopathy in dystrophin deficient mice. *BMC Cardiovasc Disord* 2011;11:20–30.
- Eagle M, Bourke J, Bullock R et al. Managing Duchenne muscular dystrophy: The additive effect of spinal surgery and home nocturnal ventilation in improving survival. *Neuromuscul Disord* 2007;17:470–475.
- Eagle M, Baudouin SV, Chandler C et al. Survival in Duchenne muscular dystrophy: Improvements in life expectancy since 1967 and the impact of home nocturnal ventilation. *Neuromuscul Disord* 2002;12:926–929.
- Nigro G, Comi LI, Politano L et al. The incidence and evolution of cardiomyopathy in Duchenne muscular dystrophy. *Int J Cardiol* 1990;26:271–277.
- Bushby K, Muntoni F, Bourke JP. 107th ENMC international workshop: The management of cardiac involvement in muscular dystrophy and myotonic dystrophy. 7th–9th June 2002, Naarden, The Netherlands. *Neuromuscular Disord* 2003;13:166–172.

- 7 Baxter P. Treatment of the heart in Duchenne muscular dystrophy. *Dev Med Child Neurol* 2006;48:163.
- 8 Duboc D, Meune C, Lerebours G et al. Effect of Perindopril on the onset and progression of left ventricular dysfunction in Duchenne muscular dystrophy. *J Am Coll Cardiol* 2005;45:855–857.
- 9 Ramaciotti C, Heistein LC, Coursey M et al. Left ventricular function and response to Enalapril in patients with Duchenne muscular dystrophy during the second decade of life. *Am J Cardiol* 2006;98:825–827.
- 10 Duboc D, Meune C, Pierre B et al. Perindopril preventive treatment on mortality in Duchenne muscular dystrophy: 10 years' follow-up. *Am Heart J* 2007;154:596–602.
- 11 Rhodes J, Margossian R, Darras BT et al. Safety and efficacy of carvedilol therapy for patients with dilated cardiomyopathy secondary to muscular dystrophy. *Pediatr Cardiol* 2008;29:343–351.
- 12 Kajimoto H, Ishigaki K, Okumura K et al. Beta-blocker therapy for cardiac dysfunction in patients with muscular dystrophy. *Circ J* 2006;70:991–994.
- 13 Viollet L, Thrush PT, Flanigan KM et al. Effects of angiotensin-converting enzyme inhibitors and/or beta blockers on the cardiomyopathy in Duchenne muscular dystrophy. *Am J Cardiol* 2012;110:98–102.
- 14 Ishikawa Y, Bach JR, Minami R. Cardio-protection for Duchenne's muscular dystrophy. *Am Heart J* 1999;137:895–902.
- 15 Jefferies JL, Eidem BW, Belmont JW et al. Genetic predictors and remodeling of dilated cardiomyopathy in muscular dystrophy. *Circulation* 2005;112:2799–2804.
- 16 Ogata H, Ishikawa U, Ishikawa Y et al. Beneficial effects of beta-blockers and angiotensin-converting enzyme inhibitors in Duchenne muscular dystrophy. *J Cardiol* 2009;53:72–78.
- 17 Biggar WD, Harris VA, Eliasoph L et al. Long-term benefits of deflazacort treatment for boys with Duchenne muscular dystrophy in their second decade. *Neuromuscul Disord* 2006;16:249–255.
- 18 Silversides CK, Webb GD, Harris et al. Effects of Deflazacort on left ventricular function in patients with Duchenne muscular dystrophy. *Am J Cardiol* 2003;91:769–772.
- 19 Markham LW, Spicer RL, Khoury PR et al. Steroid therapy and cardiac function in Duchenne muscular dystrophy. *Pediatr Cardiol* 2005;26:768–771.
- 20 Markham LW, Kinnett K, Wong BL et al. Corticosteroid treatment retards development of ventricular dysfunction in Duchenne muscular dystrophy. *Neuromuscul Disord* 2008;18:365–370.
- 21 Houde S, Filiatrault M, Fournier A et al. Deflazacort use in Duchenne muscular dystrophy: An 8-year follow-up. *Pediatr Neurol* 2008;38:200–206.
- 22 Yasuda S, Townsend D, Michele DE et al. Dystrophic heart failure blocked by membrane sealant poloxamer. *Nature* 2005;436:1025–1029.
- 23 Townsend D, Turner I, Yasuda S et al. Chronic administration of membrane sealant prevents severe cardiac injury and ventricular dilation in dystrophic dogs. *J Clin Invest* 2010;120:1140–1150.
- 24 Piccolo G, Azan G, Tonin P et al. Dilated cardiomyopathy requiring cardiac transplantation as initial manifestation of Xp21 Becker type muscular dystrophy. *Neuromuscul Disord* 1994;4:143–146.
- 25 Saito M, Kawai H, Akaike M et al. Cardiac dysfunction with Becker muscular dystrophy. *Am Heart J* 1996;132:642–647.
- 26 Berko BA, Swift M. X-linked dilated cardiomyopathy. *N Engl J Med* 1987;316:1186–1191.
- 27 Towbin JA, Hejtmancik JF, Brink P et al. X-linked dilated cardiomyopathy: Molecular genetic evidence of linkage to the Duchenne muscular dystrophy (dystrophin) gene at the Xp21 locus. *Circulation* 1993;87:1854–1865.
- 28 Townsend D, Blankinship MJ, Allen JM et al. Systemic administration of micro-dystrophin restores cardiac geometry and prevents dobutamine-induced cardiac pump failure. *Mol Ther* 2007;15:1086–1092.
- 29 Gregorevic P, Allen JM, Minami E et al. rAAV6-microdystrophin preserves muscle function and extends lifespan in severely dystrophic mice. *Nat Med* 2006;12:787–789.
- 30 Harper S, Hauser MA, DelloRusso C et al. Modular flexibility of dystrophin: Implications for gene therapy of Duchenne muscular dystrophy. *Nat Med* 2002;8:253–261.
- 31 Bostick B, Yue Y, Long C et al. Cardiac expression of a mini-dystrophin that normalizes skeletal muscle force only partially restores heart function in aged Mdx mice. *Mol Ther* 2009;17:253–261.
- 32 Mendell JR, Rodino-Klapac LR, Rosales XQ et al. Sustained alpha-sarcoglycan gene expression after gene transfer in limb-girdle muscular dystrophy, Type 2D. *Ann Neurol* 2010;68:629–638.
- 33 Mingozzi F, Hasbrouck NC, Basner E et al. Modulation of tolerance to the transgene product in a nonhuman primate model of AAV-mediated gene transfer to liver. *Blood* 2007;110:2334–2341.
- 34 Mingozzi F, Meulenberg JJ, Hui DJ et al. AAV-1 mediated gene transfer to skeletal muscle in humans results in dose-dependent activation of capsid-specific T cells. *Blood* 2009;114:2077–2086.
- 35 Wang Z, Storb R, Lee D et al. Immune responses to AAV in canine muscle monitored by cellular assays and noninvasive imaging. *Mol Ther* 2010;18:617–624.
- 36 Wu B, Xiao B, Cloer C et al. One-year treatment of morpholino antisense oligomer improves skeletal and cardiac muscle functions in dystrophic mdx mice. *Mol Ther* 2011;19:576–583.
- 37 Berry SE, Liu J, Chaney EJ et al. Multipotential mesoangioblast stem cell therapy in the *mdx/utrn*^{-/-} mouse model for Duchenne muscular dystrophy. *Regen Med* 2007;2:275–288.
- 38 Sampaolesi M, Blot S, D'Antona G et al. Mesoangioblast stem cells ameliorate muscle function in dystrophic dogs. *Nature* 2006;444:574–579.
- 39 Koh GY, Soonpaa MH, Klug MG et al. Stable fetal cardiomyocyte grafts in the hearts of dystrophic mice and dogs. *J Clin Invest* 1995;96:2034–2042.
- 40 Payne TR, Oshima H, Sakai R et al. Regeneration of dystrophin-expressing myocytes in the mdx heart by skeletal muscle stem cells. *Gene Ther* 2005;12:1264–1274.
- 41 Bridges LR. The association of cardiac muscle necrosis and inflammation with the degenerative and persistent myopathy of MDX mice. *J Neurol Sci* 1986;72:147–157.
- 42 Quinlan JG, Hahn HS, Wong BL et al. Evolution of the mdx mouse cardiomyopathy: Physiological and morphological findings. *Neuromuscul Disord* 2004;14:491–496.
- 43 Bostick B, Yue Y, Long C et al. Prevention of dystrophin-deficient cardiomyopathy in twenty-one-month-old carrier mice by mosaic dystrophin expression or complementary dystrophin-utrophin expression. *Circ Res* 2008;102:121–130.
- 44 Tinsley JM, Potter AC, Phelps SR et al. Amelioration of the dystrophic phenotype of mdx mice using a truncated utrophin transgene. *Nature* 1996;384:349–353.
- 45 Grady RM, Teng H, Nichol MC et al. Skeletal and cardiac myopathies in mice lacking utrophin and dystrophin: A model for Duchenne muscular dystrophy. *Cell* 1997;90:729–738.
- 46 Chun JL, O'Brien R, Berry SE. Cardiac dysfunction and pathology in the dystrophin and utrophin-deficient mouse during development of dilated cardiomyopathy. *Neuromuscul Disord* 2012;22:368–379.
- 47 Wang L, Kamath A, Frye J. Aorta-derived mesoangioblasts differentiate into oligodendrocytes by inhibition of the Rho kinase signaling pathway. *Stem Cells Dev* 2012;21:1069–1089.
- 48 Burkin DJ, Wallace GQ, Nicol KJ et al. Enhanced expression of the $\alpha\beta$ 1 integrin reduces muscular dystrophy and restores viability in dystrophic mice. *J Cell Biol* 2001;152:1207–1218.
- 49 Odintsov B, Chun J, Mulligan J et al. 14.1 T whole body MRI for detection of mesoangioblast stem cells in a murine model of Duchenne muscular dystrophy. *Magn Reson Med* 2011;66:1704–1714.
- 50 Odintsov B, Chun J, Berry SE. Whole body MRI followed by fluorescent microscopy analysis for detection of stem cells labeled with superparamagnetic iron oxide (SPIO) nanoparticles and Dil following intracardiac injection, skeletal muscle transplantation, or systemic delivery. In: Turksen K, ed. *Methods in Molecular Biology, Imaging and Tracking Stem Cells: Methods and Protocols*. New York, NY: Humana Press, Springer Science and Business Media, in press.
- 51 Holt P, Rhode EA, Kines H. Ventricular volumes and body weight in mammals. *Am J Physiol* 1968;215:704–715.
- 52 Menasché P. Stem cell therapy for chronic heart failure: Lessons from a 15-year experience. *C R Biol* 2011;334:489–496.
- 53 Torella D, Ellison GM, Méndez-Ferrer S et al. Resident human cardiac stem cells: Role in cardiac cellular homeostasis and potential for myocardial regeneration. *Nat Clin Pract Cardiovasc Med* 2006;3(suppl 1):S83–S89.
- 54 El-Helou V, Beguin PC, Assimakopoulos J et al. The rat heart contains a neural stem cell population; Role in sympathetic sprouting and angiogenesis. *J Mol Cell Cardiol* 2008;45:694–702.

- 55 El-Helou V, Dupuis J, Proulx C. Resident nestin⁺ neural-like cells and fibers are detected in normal and damaged rat myocardium. *Hypertension* 2005;46:1219–1225.
- 56 Scobioala S, Klocke R, Kuhlmann M et al. Up-regulation of nestin in the infarcted myocardium potentially indicates differentiation of resident cardiac stem cells into various lineages including cardiomyocytes. *FASEB J* 2008;22:1021–1031.
- 57 Béguin P, El-Helou V, Assimakopoulos J et al. The phenotype and potential origin of nestin⁺ cardiac myocyte-like cells following infarction. *J Appl Physiol* 2009;107:1241–1248.
- 58 St. John Sutton MGSJ, Sharpe N. Left ventricular remodeling after myocardial infarction. *Pathophysiol Ther Circul* 2000;101:2981–2988.
- 59 Konstam MA, Kramer DG, Patel AR et al. Left ventricular remodeling in heart failure: Current concepts in clinical significance and assessment. *JACC Cardiovasc Imaging* 2011;4:98–108.
- 60 White HD, Norris RM, Brown MA et al. Left ventricular end-systolic volume as the major determinant of survival after recovery from myocardial infarction. *Circulation* 1987;76:44–51.
- 61 Galvez BG, Sampaolesi M, Barbuti A et al. Cardiac mesoangioblasts are committed, self-renewable progenitors, associated with small vessels of juvenile mouse ventricle. *Cell Death Differ* 2008;15:1417–1428.
- 62 Minasi MG, Riminucci M, De Angelis L et al. The meso-angioblast: A multipotent, self-renewing cell that originates from the dorsal aorta and differentiates into most mesodermal tissues. *Development* 2002;129:2773–2783.
- 63 Galli D, Innocenzi A, Staszewsky L et al. Mesoangioblasts, vessel-associated multipotent stem cells repair the infarcted heart by multiple cellular mechanisms. *Arterioscler Thromb Vasc Biol* 2005;25:692–697.
- 64 Tedesco FS, Gerli MFM, Perani L et al. Transplantation of genetically corrected human iPSC-derived progenitors in mice with limb-girdle muscular dystrophy. *Sci Transl Med* 2012;4:140ra89.
- 65 Katare J, Riu F, Mitchell K et al. Transplantation of human pericyte progenitor cells improves the repair of infarcted heart through activation of an angiogenic program involving micro-RNA-132. *Circ Res* 2011;109:894–906.
- 66 Young PP, Vaughan DE, Hatzopoulos AK. Biologic properties of endothelial progenitor cells and their potential for cell therapy. *Prog Cardiovasc Dis* 2007;49:421–429.
- 67 Reffellmann T, Dow JS, Dai W et al. Transplantation of neonatal cardiomyocytes after permanent coronary artery occlusion increases regional blood flow of infarcted myocardium. *J Mol Cell Cardiol* 2003;35:607–613.
- 68 Miike T, Sugino S, Ohtani Y et al. Vascular endothelial cell injury and platelet embolism in Duchenne muscular dystrophy at the preclinical stage. *J Neurol Sci* 1987;82:67–80.
- 69 Musch BC, Papapetropoulos TA, McQueen DA et al. A comparison of the structure of small blood vessels in normal, denervated and dystrophic human muscle. *J Neurol Sci* 1975;26:221–234.
- 70 Loufrani L, Matrougui K, Gorny D et al. Flow (shear stress)-induced endothelium-dependent dilation is altered in mice lacking the gene encoding for dystrophin. *Circulation* 2001;103:864–870.
- 71 Sato K, Yokota T, Ichioka S et al. Vasodilation of intramuscular arterioles under shear stress in dystrophin-deficient skeletal muscle is impaired through decreased nNOS expression. *Acta Myologica* 2008;27:30–36.
- 72 Sander M, Chavoshan B, Harris SA et al. Functional muscle ischemia in neuronal nitric oxide synthase-deficient skeletal muscle of children with Duchenne muscular dystrophy. *Proc Natl Acad Sci USA* 2000;97:13818–13823.
- 73 Messina S, Mazzeo A, Bitto A et al. VEGF overexpression via adeno-associated virus gene transfer promotes skeletal muscle regeneration and enhances muscle function in mdx mice. *FASEB J* 2007;21:3737–3746.
- 74 D'Amore PA, Brown RH, Ku PT et al. Elevated basic fibroblast growth factor in the serum of patients with Duchenne muscular dystrophy. *Ann Neurol* 1994;35:362–365.
- 75 Fang J, Shi G, Vaghy PL. Identification of the increased expression of monocyte chemoattractant protein-1, cathepsin S, UPIX-1, and other genes in dystrophin-deficient mouse muscles by suppression subtractive hybridization. *J Cell Biochem* 2000;79:164–172.
- 76 Porter JD, Guo W, Merriam AP et al. Persistent over-expression of specific CC class chemokines correlates with macrophage and T-cell recruitment in mdx skeletal muscle. *Neuromuscul Disord* 2003;13:223–235.
- 77 Toti P, Villanova M, Vatti R et al. Nerve growth factor expression in human dystrophic muscles. *Muscle Nerve* 2003;27:370–373.
- 78 Straino S, Germani A, Di Carlo A et al. Enhanced arteriogenesis and wound repair in dystrophin-deficient mdx mice. *Circulation* 2004;110:3341–3348.
- 79 Kachinsky AM, Dominov JA, Miller JB. Intermediate filaments in cardiac myogenesis: nestin in the developing mouse heart. *J Histochem Cytochem* 1995;43:843–847.
- 80 Tomita Y, Matsumura K, Wakamatsu Y et al. Cardiac neural crest cells contribute to the dormant multipotent stem cell in the mammalian heart. *J Cell Biol* 2005;170:1135–1146.
- 81 Mokřý J, Karbanová J, Filip S et al. Phenotypic and morphological characterization of *in vitro* oligodendroglioneogenesis. *Stem Cells Dev* 2008;17:333–341.
- 82 Blau HM, Webster C, Pavlath GK. Defective myoblasts identified in Duchenne muscular dystrophy. *Proc Natl Acad Sci USA* 1983;80:4856–4860.
- 83 Webster C, Blau HM. Accelerated age-related decline in replicative life-span of Duchenne muscular dystrophy myoblasts: Implications for cell and gene therapy. *Somat Cell Mol Genet* 1990;16:557–565.
- 84 Kudryashova E, Kramerova I, Spencer MJ. Satellite cell senescence underlies myopathy in a mouse model of limb-girdle muscular dystrophy 2H. *J Clin Invest* 2012;122:1764–1776.
- 85 Cassano M, Berardi E, Crippa S et al. Alteration of cardiac progenitor cell potency in GRMD dogs. *Cell Transplant* 2012 [Epub ahead of print].
- 86 Sacco A, Mourikioti F, Tran R et al. Short telomeres and stem cell exhaustion model Duchenne muscular dystrophy in mdx/mTR mice. *Cell* 2010;143:1059–1071.
- 87 Wang JS, Shum-Tim D, Chedrawy E et al. The coronary delivery of marrow stromal cells for myocardial regeneration: Pathophysiologic and therapeutic implications. *J Thorac Cardiovasc Surg* 2001;122:699–705.



See www.StemCellsTM.com for supporting information available online.